Biomaterials 33 (2012) 8757–8770

Contents lists available at SciVerse ScienceDirect

Biomaterials

journal homepage: www.elsevier.com/locate/biomaterials

Molecular simulation of flavin adenine dinucleotide immobilized on charged single-walled carbon nanotubes for biosensor applications

Guang Yang [a,c,1], Zhengzhong Kang [b,1], Xuesong Ye [a,c,*], Tao Wu [b,**], Qin Zhu [a,c]

[a] College of Biomedical Engineering & Instrument Science, Zhejiang University, PR China
[b] Soft Matter Research Center and Department of Chemistry, Zhejiang University, PR China
[c] Key lab of Biomedical Engineering of Ministry of Education, Zhejiang University, Hangzhou 310027, PR China

ARTICLE INFO

Article history:
Received 2 August 2012
Accepted 23 August 2012
Available online 11 September 2012

Keywords:
Flavin adenine dinucleotide
Glucose oxidase
Molecular simulation
Charged single-walled carbon nanotubes

ABSTRACT

The reconstitution of apo-glucose oxidase (apo-GOx) on single-walled carbon nanotubes (SWNTs) functionalized with the cofactor, flavin adenine dinucleotide (FAD), greatly improved electron transfer turnover rate of the redox reactions in glucose sensing with glucose sensors. The research reported here is aimed to better understand molecular details of affection of the charging SWNT to the conformational changes of FAD, in order to find a rational design and selection scheme of SWNT which is suitable for the FAD and apo-GOx to perform their reconstitution. In this report, molecular simulations of FAD functionalized differently charged SWNTs were carried outin an aqueous environment, with counterions to maintain total charge neutrality. The conformation and orientation changes were observed by both trajectory and quantitative analyses. The simulation results showed that in both uncharged and positively charged SWNT situations, FAD adsorbed onto SWNT at the end of the simulations, which increased the steric resistance of molecules and hindered the reconstitution of apo-GOx and FAD to some degree. By contrast, FAD functionalized negatively charged SWNT maintained its original conformation largely. In addition, negatively charged SWNT may be the best choice for electron transfer mediator for the reconstitution of apo-GOx on relay-cofactor units associated with electrodes.

1. Introduction

During the past few decades, carbon nanotubes (CNTs) have attracted wide attention owing to their unique structures and properties (optical, mechanical, electronic, thermal etc.) since their discovery in 1991 [1] and recent studies have demonstrated the use of single-walled carbon nanotubes (SWNTs) in nanodevices and sensors [2–6]. As a promising biomaterial, biomolecules covalently functionalized SWNTs have been intensively investigated [1,7–11] for several proteins-material systems, for example, glucose oxidase (GOx). Redox sites in glucose GOx lack direct electrical contact with electrodes due to the insulation of the redox center by the GOx, so that electron transfer between the enzyme redox center and electrodes cannot be detected accurately [12]. The investigations showed that electron transfer turnover rate of the apo-GOx reconstituted system was greatly improved due to the existence of the SWNTs which acted as conductive nanoneedles that electrically wired the enzyme redox-active site to the transducers surface by Itamar Willner et al via an actual system [13]. Reconstitution of apo-GOx with semi-artificial FAD cofactor comes out as a solution that the most difficult challenge is how to maintain the activity of the enzyme and make electron transfer from the catalytic center to electrodes quickly and efficiently [14–17].

It has been proved that doping in CNTs can enhance the electrical conductivity in the systems [18–20]. Carbon nanotubes can be doped in various ways, which can change the electrical properties of CNTs, such as by doping nanotubes with p-type dopants to produce positively charged nanotubes and by doping n-type dopants to produce negatively charged nanotubes [21–24]. Doping of CNTs can be realized by the substitution of carbon atoms with foreign atoms such as phosphorus, boron or nitrogen; or by adsorption of some molecules with appropriate functional groups, such as NADH and viologen, on the nanotubes [23,25–30]. And the doping type is decided by the direction of electrons transferring between carbon nanotubes and dopants. When the electrons transfer from dopants to CNTs, which makes the Fermi level shifted toward the conduction band, the nanotubes are n-type doping.

* Corresponding author. Key lab of Biomedical Engineering of Ministry of Education, Zhejiang University, Hangzhou 310027, PR China.
** Corresponding author.
E-mail addresses: yexuesong@zju.edu.cn (X. Ye), tao_wu@zju.edu.cn (T. Wu).
[1] These authors contributed equally to this work.

0142-9612/$ – see front matter © 2012 Elsevier Ltd. All rights reserved.
http://dx.doi.org/10.1016/j.biomaterials.2012.08.053

On the contrary, when the electrons transfer from CNTs to dopants, which make the Fermi level shifted toward the valence band, the nanotubes are p-type doping. It has been proved that chemical doping can substantially increase the density of free charge carriers and enhance the electrical conductivity in the systems based on carbon nanotubes both in experiments and molecular simulations [18–20].

But research about how the charged carbon nanotubes affect immobilization of biomolecule is still quite few. In order to solve this problem, we choose flavin adenine dinucleotide, a mostly discussed biomolecule in glucose biosensors, as our object to reveal how the different electrical properties carbon nanotubes affect the conformational and orientation changes for a rational design of biosensors. These investigations above make it possible to reconstitute GOx and maintain its activity properly in the experiment and turn the 'electroenzyme' into reality. Nevertheless, the atomic details of fundamental interactions between SWNTs and FAD at molecular level are still unclear, owing to the limitation of the experimental methods. For example, the details of conformation changes of FAD due to its combination with SWNTs cannot well explored via these techniques, which are of great importance to have a better understanding of the reconstitution of apo-GOx with semi-artificial FAD cofactor. Molecular dynamics (MD) simulations can provide insights into the ultimate details of fundamental interactions at molecular level and it is also an excellent method for imaging in bionanotechnology, covering the space scale rather well and the time scale up to many nanoseconds. They can be utilized to study specific properties of a molecular system and also perform more easily than experiments on actual systems most of the time. Of course, experiments also play an essential role in promoting simulation methodology and they verify the errors of simulations and provide more accurate parameters for the semi-empirical methods.

In this paper MD and SMD simulation results for conformational changes of FAD covalently functionalized differently charged SWNTs in an aqueous solution were reported. The questions we address here are focused on a) molecular details of affection of the charging SWNT to the conformational changes of FAD; b) rational design and selection of SWNT which is suitable for the FAD and apo-GOx to perform their reconstitution. Our molecular simulations provide a detailed look at FAD-SWNT interactions for a simple model systems consisting of a FAD covalently functionalized differently charged SWNTs in a solution of water and counterions.

2. Material and method

GOx, a homodimer with a molecular weight of 160kDalton, can be decomposed into an apo-GOx and an embedded coenzyme, FAD. The x-ray structure of FAD of GOx was derived from the protein data bank (ID code 1GAL) [31]. In this study, all MD simulations were performed by NAMD [32] program with the force field CHARMM27 [17]. The FAD coenzyme was selected to explore the dynamics behaviors when FAD functionalized charged or uncharged SWNTs. We have generated an 'armchair' SWNT, 1 nm in diameter and 3.45 nm in length containing 600 carbon atoms using the program Tubegen [31]. The FAD was covalently linked to a $-CH_2-CH_2-NH_2$ group according to the literature [13]. Then the $-CH_2-CH_2-NH_2$ group was covalently linked to a −COOH group which covalently functionalized constructed SWNTs. The whole structure of the FAD$-CH_2-CH_2-$NH−CO−SWNT molecular system is displayed in Fig. 1c.

Our simulations were performed in the following manners:

a) The energy minimization and energy equilibration of FAD were performed. The FAD was solvated in water molecules, with a typical starting simulation cell of about $18.82 \times 19.23 \times 31.44$ Å^3. The system underwent a 5000 steps energy minimization. A molecular dynamics run of the system was carried out for 200 ps until the Root-Mean-Square Deviation (RMSD) of FAD fluctuated around a constant value, which indicated that FAD came to an equilibrium status. Then the conformational orientation of FAD was used as the initial status for the FAD$-CH_2-CH_2-$NH−CO−SWNT hybrid system.

b) Three SWNT models [31] with nominal charges on each carbon atom of $q = 0.00$e, $q = +0.10$e, and $q = -0.10$e were built. Thus, the total charges on the nanotubes were 0e, +60e, and −60e, respectively. We covalently linked the $-NH_2$ terminal of $-CH_2-CH_2-NH_2$ group to the −COOH group which covalently linked to each SWNTs. Then we used FAD to link the other terminal of $-CH_2-CH_2-NH_2$ group. After that, we solvated the hybrid system in a TIP3 water box of size of $44.76 \times 35.23 \times 79.34$ Å^3. Then we added 60 sodiums to the negatively charged hybrid system and 60 chlorines to the positively charged hybrid system to maintain the charge of these systems neutrality.

c) Thirdly, a 5000 steps energy minimization of the whole system (containing the SWNT, $-CH_2-CH_2-NH_2$, FAD, counterions and water molecules) was performed. Then 18 ns MD runs were done. The main goal of the simulations focused on the dynamic features of the FAD and how the different electrical properties of SWNT affected the behaviors of FAD in the MD runs.

We employed the CHARMM27 force field [17], and the force field of the cofactor FAD was empirically constructed from a combination of FMN and ATP in GROMACS [32]. The parameters for the Lennard-Jones potential for the cross interactions between non-bonded atoms were obtained from the Lorentz–Berthelot combining rule. All simulations were performed with a time step of 2 fs, and a cut-off was set with a switching function starting at a distance of 10 Å and reaching zero at 12 Å. A particle mesh Ewald (PME) summation was used to calculate the long-range electrostatic interactions, with a cut-off distance of 12 Å for the separation of the direct and reciprocal space. During the MD simulations, the Langevin method was used to ensure a constant temperature of 310 K and a constant pressure of 1 atm. Periodic boundary conditions were applied for all the simulations. Visualization and analysis of the configurations were performed with the VMD [33] packages and the utility packages included in NAMD [32]. And there are some parameters which do not exist in the standard parameter files, so we have built some parameters for the hybrid system according to existing parameters of the same structure.

The time-dependent interaction energy $E_{\mathrm{int}}(t)$ for the systems in MD simulations is defined by the Equation (1):

$$E_{\mathrm{int}}(t) = E_{\mathrm{SWNT+FAD}}(t) - E_{\mathrm{SWNT}}(t) - E_{\mathrm{FAD}}(t) \tag{1}$$

where $E_{\mathrm{int}}(t)$ stands for the total interaction energy between the FAD and the SWNT at time t during the MD simulation, and $E_{\mathrm{SWNT+FAD}}(t)$, $E_{\mathrm{SWNT}}(t)$, $E_{\mathrm{FAD}}(t)$ are the total potential energy of the SWNT plus FAD, of the SWNT, and of the FAD at time t during the MD simulation, respectively. The vdW interaction energy and the electrostatic interaction energy were defined similarly to the total interaction energy [16,34]. These data were saved every 500 steps and derived from the saved frames in the 18 ns simulations.

After the MD simulations, we went through steered molecular dynamics (SMD) simulations to understand the kinetics and the structural determinants of the all three systems. In principle, SMD simulation is carried out by attaching a harmonic restraint to one or more atoms in the system, and then varying either the stiffness of the restraint or the position of the restraint to pull the atoms along. In the constant velocity pulling simulation, the SMD atom is attached to a dummy atom via a virtual spring and the dummy atom moves at a constant velocity and then the force between them is measured using:

$$\vec{F} = -\nabla U$$

$$U = \frac{1}{2}k[vt - (\vec{r} - \vec{r}_0)\cdot\vec{n}]^2 \tag{2}$$

where U is the potential energy, k stands for the spring constant, v is the pulling velocity, t is the time, $\vec{r}$ and $\vec{r}_0$ are the actual position and the initial position of the SMD atom respectively, and $\vec{n}$ represents the direction of pulling.

In our cases, all atoms of SWNTs were constrained and all atoms in the FAD were selected to be the SMD atoms except hydrogen atoms. The direction of constant velocity was set to be along the central axis of the SWNT toward the side connected with FAD. The spring constant must be high enough that the local unbinding potential is sampled, but must not be too high or the measured force will be dominated by noise. At last, the spring constant was set to be 30 kJ mol^{-1} Å^{-2} and the pulling velocity was fixed at 1×10^{-4} Å fs^{-1} to get good SMD observation window.

3. Results and discussions

The glucose oxidase enzyme (GOx) is an oxido-reductase that catalyzes the oxidation of glucose to hydrogen peroxide and D-glucono-δ-lactone. GOx is a flavoenzyme with molecular weight about 160,000 Da, which includes two identical subunits, each containing a strongly non-covalently associated FAD cofactor unit [35]. In order to function as a catalyst, GOx requires a cofactor, flavin adenine dinucleotide (FAD), which is a common component in

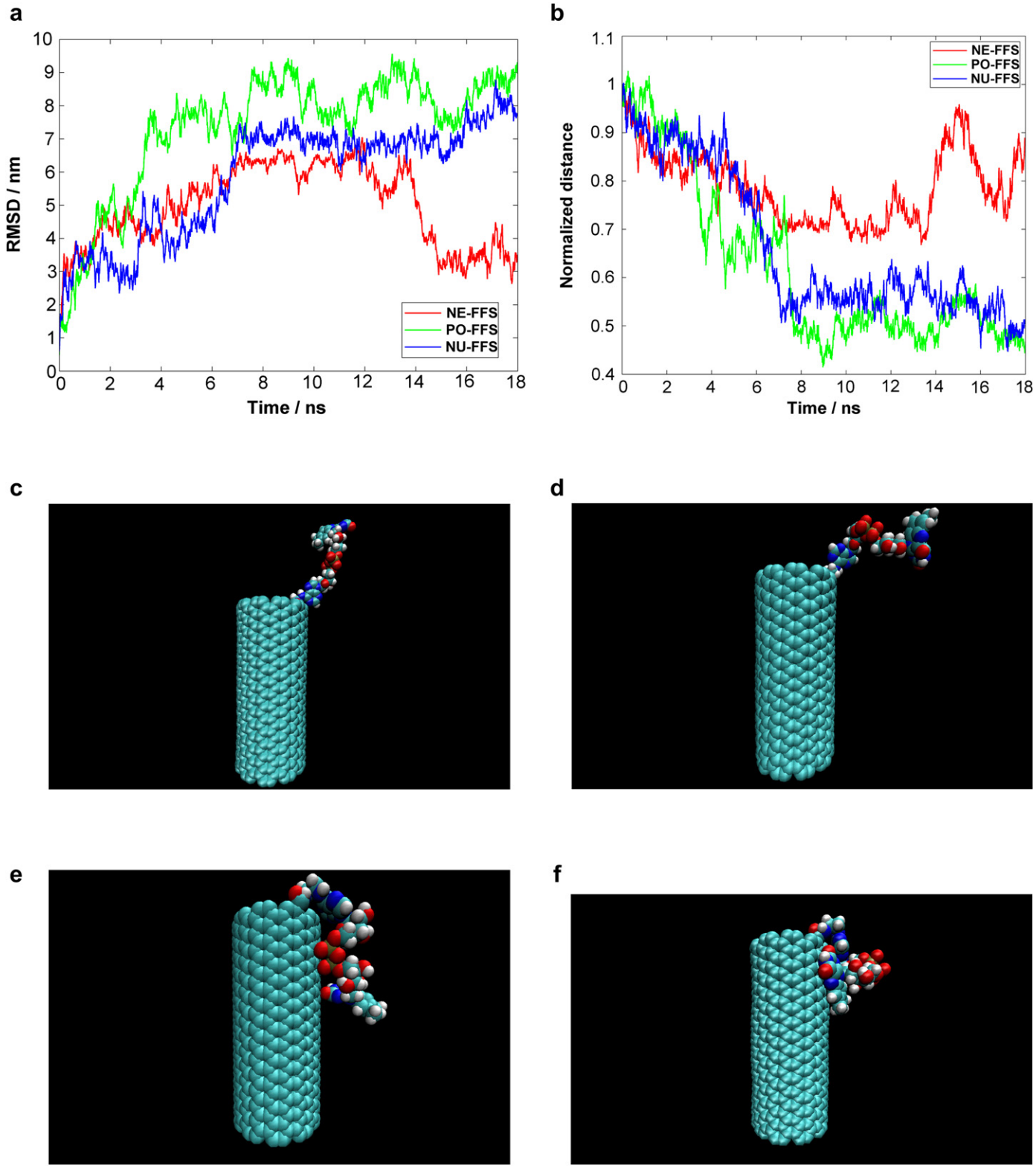

Fig. 1. (a)RMSD of three different systems in 18 ns MD simulations. b)Normalized distance between the COM of the FAD and the three different charged SWNT .Green line displays that the normalized distance between the COM of the FAD and the positively charged SWNT changed by time; red line shows that the normalized distance between the COM of the FAD and the negatively charged SWNT; blue line indicates that the normalized distance between the COM of the FAD and the uncharged SWNT.(c) Side view of the initial state of FAD before minimization and MD simulations in three systems. Side views of state of FAD in (d) NE-FFS, (e) PO-FFS, and (f) NU-FFS on the varied charged SWNTs. The whole systems are displayed in VDW model. Water molecules and counterions are not displayed here for clarity. (For interpretation of the references to colour in this figure legend, the reader is referred to the web version of this article.)

biological oxidation-reduction (redox reactions). Redox reactions involve a gain or loss of electrons from a molecule. In the GOx-catalyzed redox reaction, FAD works as the initial electron acceptor and is reduced to $FADH_2$. Then $FADH_2$ is oxidized by the final electron acceptor, molecular oxygen (O_2), which can do so because it has a higher reduction potential. O_2 is then reduced to hydrogen peroxide (H_2O_2).

Redox sites in GOx lack direct electrical contact with electrodes due to the insulation of the redox center by the GOx, so that electron transfer between the enzyme redox center and electrodes cannot be detected accurately [12]. The challenge above led to the development of various methods to establish electrical communication between redox-enzymes and electrode supports using electron transfer mediators, and some progress has been achieved, such as tethering of redox-relay units to enzymes associated with electrodes [36–38], the immobilization of enzymes in redox-polymers [39], and the reconstitution of apo-enzymes on relay-cofactor units associated with electrodes [40].

As a very important coenzyme, FAD acts as an electronic transfer agent in the redox reaction. The methods of the reconstitution of the apo-GOx units on the FAD covalently linked to SWNT were found by Itamar Willner and his co-workers [38,39]. They revealed that SWNT acted as a nano-connector which electrically connected the active site of enzyme with the electrode. Their methods can greatly make the electronic insulation properties of enzyme better and improve the electronic transfer efficiency. In our investigations, according to the experiments [38,39], we built a FAD–CH_2–CH_2–NH–CO–SWNT hybrid system and solvated the hybrid system in a water box with counterions to maintain the whole system neutrality and used MD simulations to investigate how the differently charged SWNTs affected the conformation changes of FAD. The focused problems of our investigations address as follows:

a) Are the conformations and orientations of FADs different when they functionalized differently charged SWNTs, and how?
b) What's the major reason that FADs performed different conformation and orientation changes in all the MD simulations?
c) Which kind of SWNT is more suitable for the FAD and apo-GOx to perform their reconstitutions?

3.1. Conformation and dynamics of FAD

In the following discussion, the abbreviations NU-FFS, PO-FFS and NE-FFS are used to represent the systems of FAD functionalized neutral, positively charged, and negatively charged SWNTs. Root-Mean-Square Deviation (RMSD) are series of important parameters, which can measure the difference between the structures. We investigated out the RMSD for the whole three hybrid systems, which are shown in Fig. 1a.

During the last 1 ns of all simulations, the RMSDs of all these systems fluctuate around rather stable values, which implies that stable states were achieved for all the systems investigated. However, the value of RMSD of FAD functionalized positively charged SWNT is larger than the other two systems, leading to a fact that the orientation of this hybrid system changed the most among these three systems. The RMSD of all the systems increases in the first 7 ns due to the conformational change under the static electricity attraction and conjugative effect. The RMSD in both PO-FFS and NU-FFS oscillates around 8 nm while the RMSD of the NE-FFS system oscillates around 3 nm in the end of the simulation. Meanwhile, the RMSD values of NE-FFS system are much smaller than the other two systems, referring the orientation of the hybrid system changed less in the NE-FFS system. At the same time, the RMSD changes of the NE-FFS system are sharper than the other two systems, which imply that the conformational changes of the NE-FFS system are much larger than the other two systems.

In our MD simulations, we investigated the conformation and orientation changes of the FAD covalently functionalizing differently charged SWNTs. The side view of initial and final states of the hybrid systems is shown in Fig. 1. Fig. 1c shows the initial state of the three systems before the minimization and MD simulation, and FAD functionalized differently charged SWNTs after MD simulations are shown in Fig. 1d–f.

We investigated the normalized center of mass (COM) distances between the FAD and that of SWNTs in three different systems as shown in Fig. 1b. There are some fluctuations for the normalized COM distance during the 18 ns MD simulation, implying that SWNTs induce conformational changes and structural rearrangement of FAD and showing unique nature. We found, in the 18 ns simulation, the normalized COM distance between the FAD and the positively charged and uncharged SWNTs slowly got shorter during the first 8 ns and fluctuated around 0.5 nm in the rest simulation as shown in Fig. 1b. From the above data, we can deduce that FAD has the tendency of adsorbing onto the exterior surface of both positively charged and uncharged SWNTs but for different reasons which will be discussed below. As the media of electron transfer in the redox reaction, isoalloxazine is almost the key part in FAD. With strong electronegativity, phosphate radical groups are also of great importance. So the normalized COM distance between isoalloxazine, phosphate radical groups and charged or uncharged SWNT are also very essential. Certain investigation on important residues has been done to study the conformational changes of these systems.

For the NU-FFS system, FAD slid to the exterior surface of uncharged SWNT due to the conjugative effect. In our case, isoalloxazine, which is a kind of heterocyclic structure, was driven to adsorb onto the exterior surface of uncharged SWNT by conjugative effect, causing the reduction of the normalized COM distance between FAD and SWNT from 0.9 to 0.5 approximately as shown in Fig. 2. By analyzing the trajectory files, during the first 4 ns, FAD performed a random movement due to the collision by the water molecules around it. And then, at 5 ns, isoalloxazine began to adsorb onto the adenine of the FAD due to conjugative effect until isoalloxazine adsorbed onto SWNT swiftly because of a stronger conjugative effect at 7 ns, which is mirrored as a sudden drop in curve of the illustration. Obviously, the values of the normalized COM distance between phosphate radical groups and the uncharged SWNT are always larger than the COM distance of FAD and isoalloxazine, which reflected that phosphate radical groups couldn't adsorb onto the exterior surface of uncharged SWNT, leading FAD to form a 'U' shape and adsorb onto the SWNT during the whole adsorption. We also investigated that the adenine adsorbed onto the uncharged SWNT in the last 1 ns. The adsorption of FAD and the uncharged SWNT stayed stable till the end of the simulation with a normalized distance oscillates around 0.6 as shown in Fig. 2. And the conformation changes of the NU-FFS system in 18 ns MD simulation in time order is shown in Fig. 2.

And for the PO-FFS system, SWNT and FAD were attracted by each other, causing the reduction of the COM distance between FAD and the SWNT as well. With analysis of the trajectory files, the collision of water molecules induces the random conformational change of FAD and FAD had tendency to move closer to the SWNT in the first 4 ns while the normalized distance has a reduction from 1 nm to 0.8 nm. With the oscillation of the normalized distance around 0.7 nm, FAD stayed stable from 3.7 ns to 7 ns. Then, the curves of normalized COM distance between FAD, isoalloxazine, phosphate radical groups and SWNT drop into much lower values, implying the whole FAD got much closer to the positively charged SWNT as shown in Fig. 3. Caused by static electricity attraction with

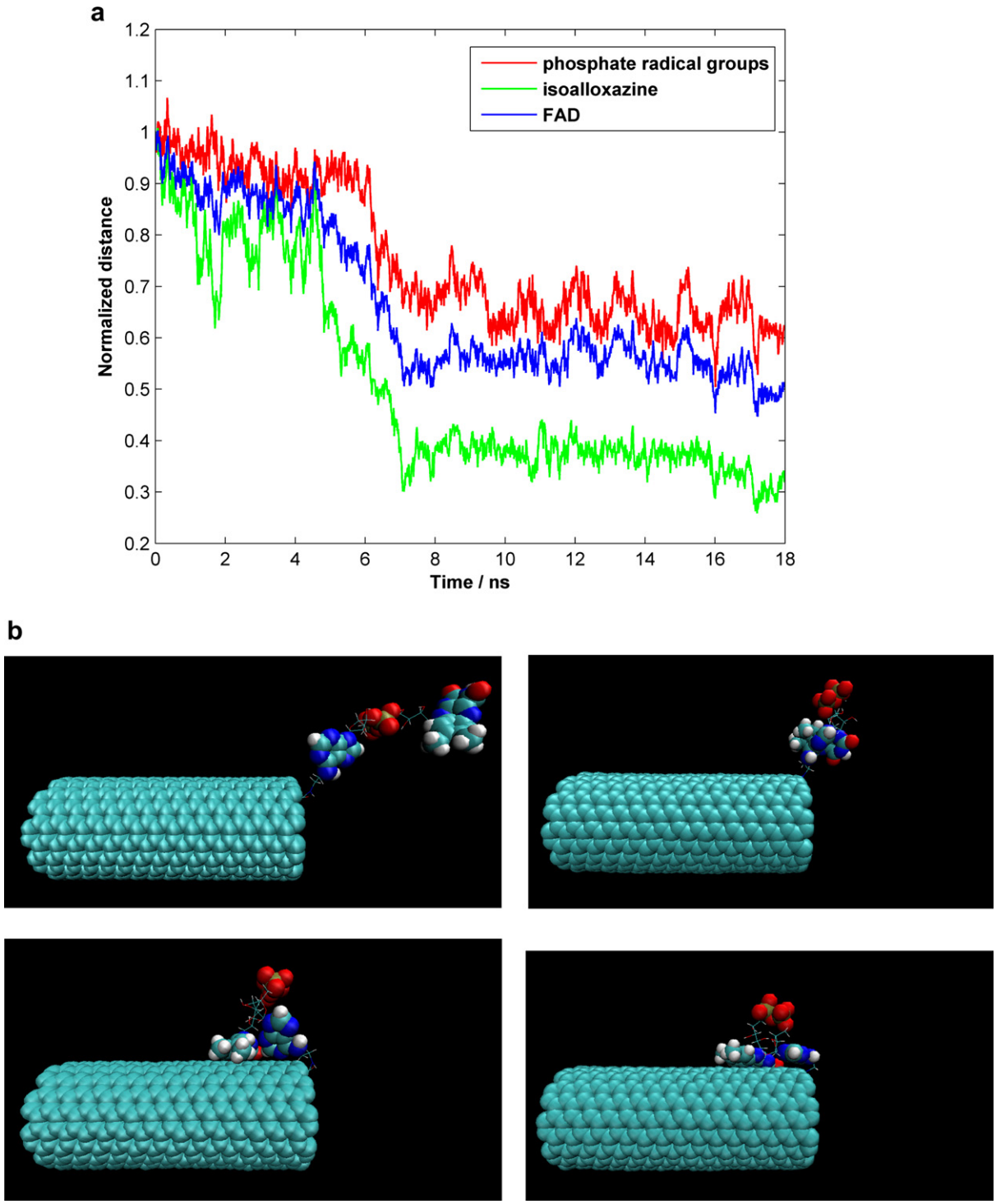

Fig. 2. (a) Distance between the FAD and the uncharged SWNT during the simulation. (b) Snapshots of the NU-FFS system (the SWNT, adenine, phosphate radical groups and isoalloxazine displayed by VDW model while other parts of the system displayed by line model) during the simulation. Water molecules and counterions are not displayed here for clarity.

positively charged SWNT, FAD began to slide toward SWNT and adsorbed onto the SWNT at about 8 ns. Led by phosphate radical groups, FAD adsorbed onto SWNT at 10 ns and stayed this state till the end of the simulation and the isoalloxazine slightly slid away from exterior surface of SWNT due to steric hindrance.

As for the NE-FFS system, the FAD conformation changing process was quite different during the 18 ns MD simulation. First of all, unlike the NU-FFS system and PO-FFS system described above, the normalized COM distance between FAD and the SWNT varied from 1 to 0.9, which didn't decrease that much compared with the other systems. It reveals that the FAD stayed almost the same distance from the SWNT in the end of the simulation. In the NE-FFS itself, the normalized COM distance between the phosphate radical groups and the SWNT is always longer than the distance between the COM of isoalloxazine or FAD and that of the SWNT as shown in Fig. 4. It implies that the phosphate radical groups are further away

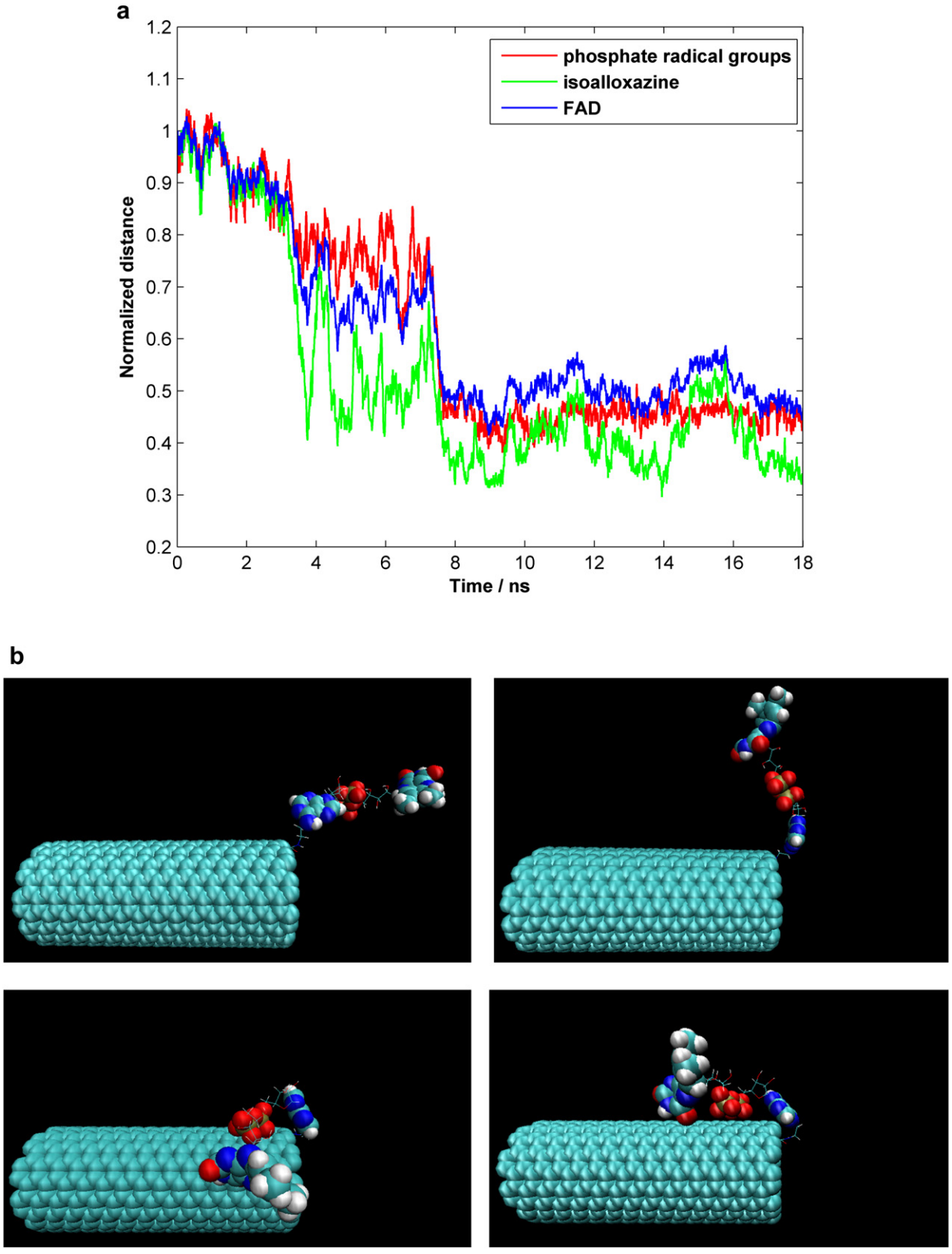

Fig. 3. (a) Distance between the FAD and the positively charged SWNT during the simulation. (b) Snapshots of the PO-FFS system (the SWNT, adenine, phosphate radical groups and isoalloxazine displayed by VDW model while other parts of the system displayed by line model) during the simulation. Water molecules and counterions are not displayed here for clarity.

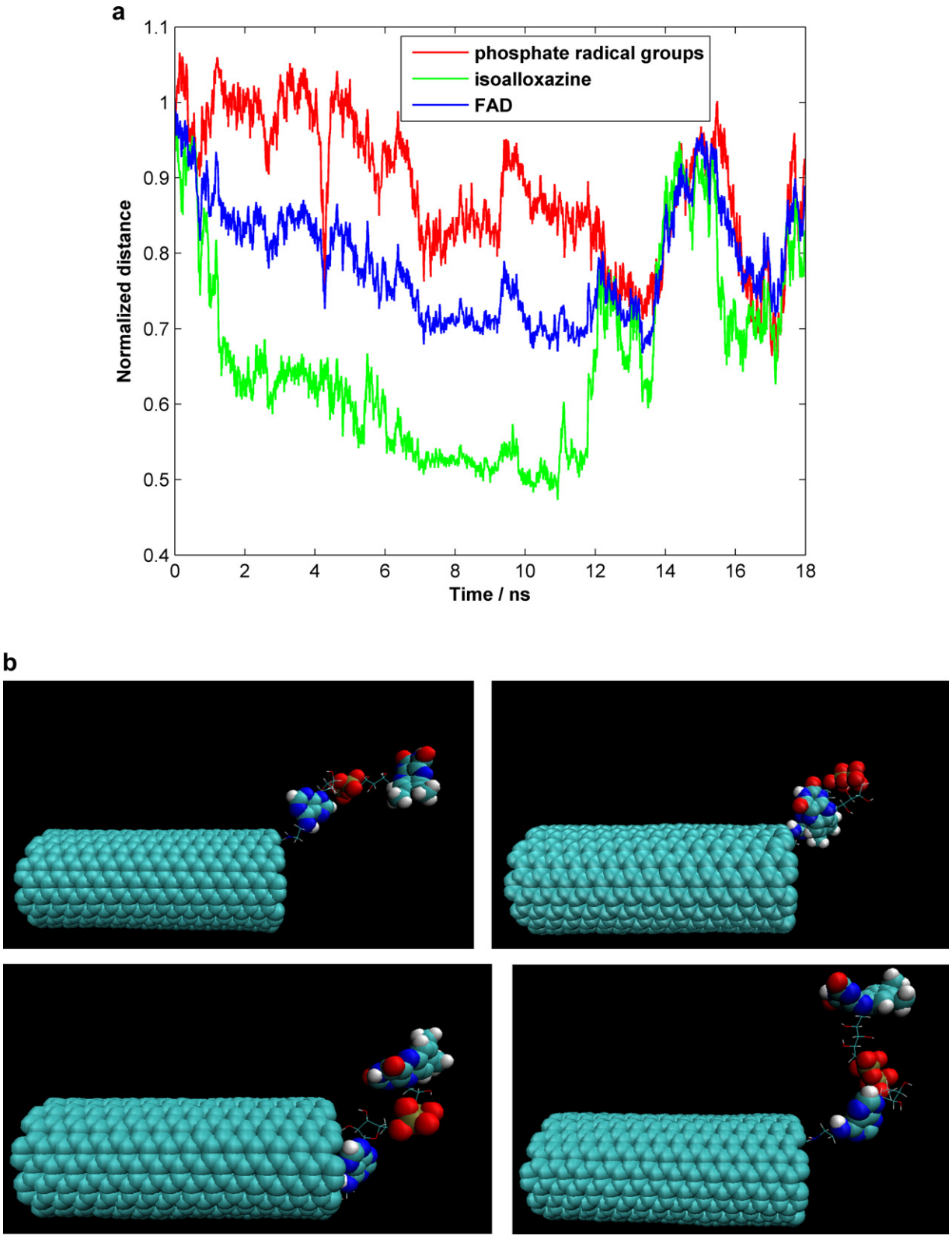

Fig. 4. (a) Distance between the FAD and the negatively charged SWNT during the simulation. (b) Snapshots of the NE-FFS system (the SWNT, adenine, phosphate radical groups and isoalloxazine displayed by VDW model while other parts of the system displayed by line model) during the simulation. Water molecules and counterions are not displayed here for clarity.

from the SWNT than FAD because of the existence of negative charges of phosphate radical groups in FAD and negative charges on SWNT. It means that phosphate radical groups and the SWNT were mutually exclusive with each other due to the same kind of charges. In more details, FAD was driven to move randomly by the collision of the water molecules from 0 ns to 1.5 ns. Then at 2 ns, the phosphate radical groups moved away from the SWNT by the electrostatic interaction as mentioned above, making the ribitol

severely distort and isoalloxazine move to adenine to form conjugate structure. And the next step, from 1.5 ns to 11 ns, the conjugate structure stayed stable. In the rest of the simulation, the normalized COM distance between isoalloxazine and the SWNT appeared to become longer and form a peak at about 0.8 while isoalloxazine and adenine stopped the adsorption and detached from each other at about 12 ns as shown in Fig. 4. And FAD began to extend slightly until it stretched violently at 14 ns, forming the second but bigger normalized distance peak approximately around 0.8 in the curve of Fig. 4. In addition, FAD performed random movement again from 14 ns till the end of the simulation with a 0.9 normalized COM distance between itself and the SWNT.

3.2. Physical properties of protein on charged SWNTs

In order to quantitatively study the dominant interaction between the model peptide and the charged CNTs, the total interaction energy, the vdW interaction energy, and the electrostatic interaction energy between FAD and the SWNTs during the simulation process were calculated. These data were derived from 18 ns simulations of the NU-FFS, PO-FFS, and NE-FFS systems, respectively. Fig. 5a shows the total interaction between the FAD and the neutral SWNT during the simulation. As presented above, in the neutral SWNT model there are no net charges on carbon atoms, so the curve could also be considered as the vdW interaction energy change during the simulation. There are some flats and barriers in this curve. In other literature [16,41,42], the researchers also found that the system which contained aromatic rings possessed a very strong interaction between biological molecules and SWNTs because of the conjugative effect between the heterocyclic and the ring structure of the SWNT. The conjugative effect reduced the system energy and made the system much more stable. After adjusted its own orientation, FAD finally adsorbed onto the SWNT, creating the vdW interaction energy drop from -3.4 kJ mol^{-1} to -27.0 kJ mol^{-1} around 6 ns with the reduction of the value of normalized distance as shown in Fig. 2a. There appears a vdW interaction peak around -12.9 kJ mol^{-1} since the isoalloxazine, which is a kind of heterocyclic structure, still adsorbed onto the adenine due to conjugative effect and the energy decreased to around -27.1 kJ mol^{-1} when isoalloxazine finally adsorbed onto the SWNT for the same reason at 9.9 ns. Then the value of vdW interaction energy fluctuates around certain values until adenine adsorbed onto the SWNT as well at 17 ns, making the vdW interaction energy dropped from -21.1 kJ mol^{-1} to -32.3 kJ mol^{-1}. In the stable state at the end of the 18 ns simulation of the NU-FFS system, the time-averaged total interaction energy fluctuates around a rather stable value of -34.4 kJ mol^{-1}. As in literature [9,17,41], SWNT is highly hydrophobic, so the hydrophilic phosphate radical groups didn't bind to the hydrophobic uncharged SWNT because of the different polarity as shown in Fig. 2. The main reason that FAD adsorbed onto the SWNT is conjugative effect, which is in line with the previous research that DNA didn't adsorb onto the uncharged SWNT [17].

As the electrostatic interaction is the dominant part in the FAD adsorption onto positively charged SWNT, as analyzed above, the effect of the charged groups on the FAD adsorption is considered to be of great importance. Therefore, the distances between the positively charged SWNT and FAD, isoalloxazine, phosphate radical groups respectively during the adsorption process were also plotted in Fig. 3a. Both phosphate radical groups and FAD moved closer to the positively charged SWNT as the time approaches 4.9 ns. Meanwhile, the electrostatic interaction energy gradually decreases to -141.8 kJ mol^{-1} or so, while the vdW interaction energy at this time is around -3.2 kJ mol^{-1}, as shown in Fig. 5b. From 4.9 ns to 7 ns, distances sharply fluctuate, which is caused by

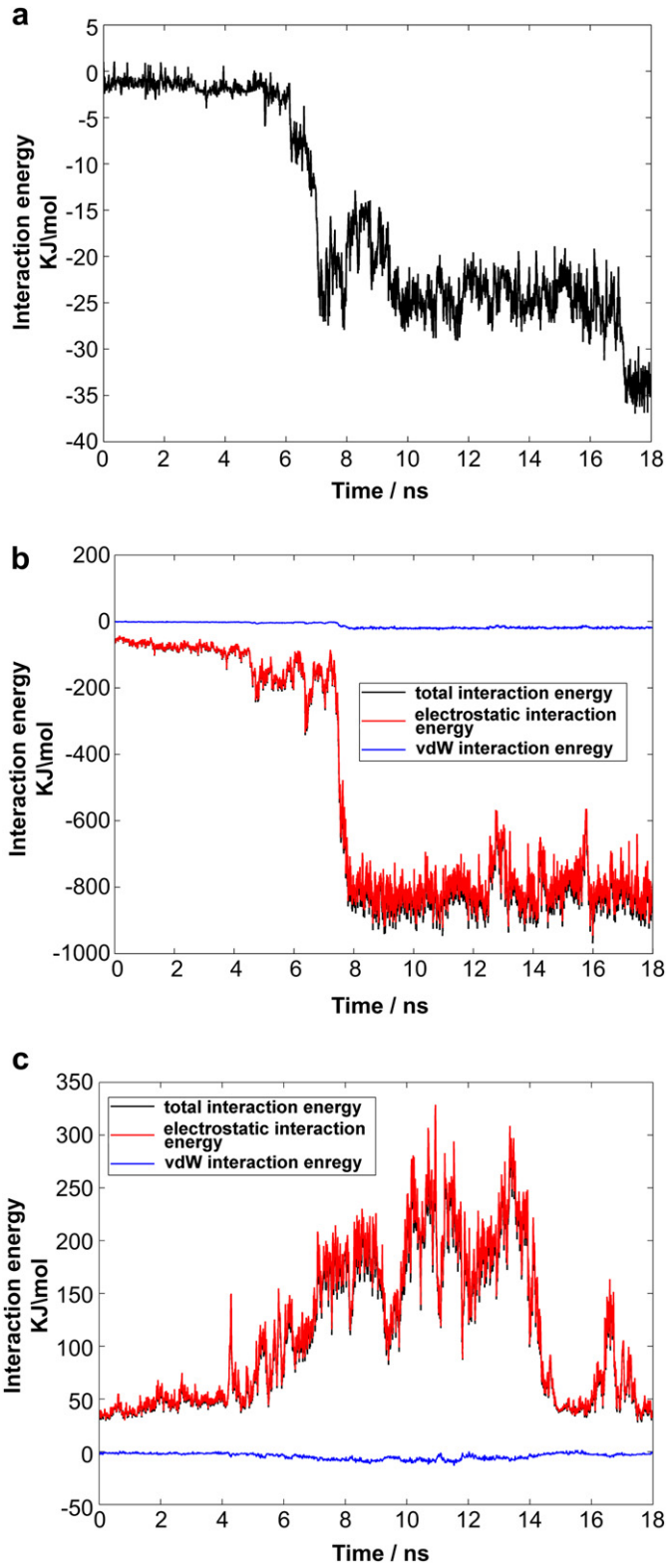

Fig. 5. (a)The total interaction energy between FAD and the uncharged SWNT during the simulation.(b)The total, vdW and electrostatic interaction energies between FAD and the positively charged SWNT during the simulation.(c)The total, vdW and electrostatic interaction energies between FAD and the negatively charged SWNT during the simulation.

the self-adjustment of the FAD conformation. During this period, the electrostatic interaction between the FAD and the SWNT sharply fluctuates, due to the phosphate radical groups. With total interaction and electrostatic interaction energy dropping down to −831.3 kJ mol^{-1} and −808.5 kJ mol^{-1} respectively, FAD started to adsorb onto the SWNT led by the electrostatic attraction from phosphate radical groups and positively charged SWNT when time approached at 8 ns. In Fig. 5b, the total, vdW, and electrostatic interaction energies between the FAD and the positively charged SWNT during the simulation are displayed. It is obvious that the total interaction energy (black line) and electrostatic interaction energy (red line) curves have very similar trends. The vdW interaction (blue line) gradually decreases during the adsorption process, but the fluctuation is much smaller than that of the total interaction energy, which implies that the vdW interaction contributes a small part of the total interaction. At the final stable state, the total, vdW and electrostatic interaction energies fluctuate around the time-averaged values of −826.9, −19.1, and −807.9 kJ mol^{-1}, respectively, and the contribution of the electrostatic interaction to the total is about 97.7%. The snapshots of phosphate radical groups during the simulation were plotted in Fig. 3b and give a direct view of the distances between the phosphate radical groups and the positively charged SWNT. This phenomenon implies that the distance between the negatively charged phosphate radical groups and the positively charged SWNT determines the strength of electrostatic interaction between the FAD and the SWNT, and hence determines the strength of the attraction from the SWNT in the adsorption process, as the electrostatic interaction plays a key role in the PO-FFS system. Simultaneously, our simulation results are in accordance with the research work of Zhao and Johnson [17].

As the electrostatic interaction is the dominant part in the FAD adsorption onto positively charged SWNT, as analyzed above, the effect of the charged groups on the FAD adsorption is considered to be of great importance. Therefore, the distances between the negatively charged SWNT and FAD, isoalloxazine, phosphate radical groups respectively during the adsorption process were also plotted in Fig. 4a. In the first 2 ns, as analyzed with the trajectory files, isoalloxazine tried to form the conjugate structure with AMP, forcing ribitol to bend and move closer to SWNT swiftly with a 0.6 normalized distance at 2.2 ns. Driven by isoalloxazine, phosphate radical groups moved closer to the negatively charged SWNT with a normalized distance decreased to 0.6 as the time approaches 0.9 ns and created a small peak 57.8 kJ mol^{-1} in the electrostatic interaction energy curve as shown in Fig. 5c. The reason why this peak is small is that the distance between phosphate radical groups and SWNT was not so close to form strong electrostatic interaction. Randomly moving till 4.28 ns, phosphate radical groups were much closer to the SWNT with a 0.74 normalized distance, and created strong electrostatic interaction energy around 149.7 kJ mol^{-1}. In addition, this electrostatic interaction energy forced phosphate radical groups to move away from the SWNT back to a 1.0 normalized distance at 4.5 ns. By the attraction of the deep potential well of the SWNT, this conjugate structure moved closer to the SWNT. Meanwhile, with the same kind of charge, phosphate radical groups and the negatively charged SWNT created stronger and stronger electrostatic interaction energy in this circumstance. And the electrostatic interaction energy increased so greatly to form a noticeable peak around 225.9 kJ mol^{-1} at 9 ns, which forced the whole FAD to move away from the SWNT as displayed in Fig. 4. As the whole FAD moved away from the SWNT, the electrostatic interaction energy decreased and formed a 101.0 kJ mol^{-1} valley in the energy curve at 9.46 ns. Then the electrostatic interaction energy raised the highest peak around 328.7 kJ mol^{-1} while the FAD kept moving close to the SWNT. And isoalloxazine couldn't bear this strong electrostatic force and started to make conformation change. Isoalloxazine moved away from the SWNT to a 0.79 normalized distance, making FAD stretch and the electrostatic interaction energy decrease around a low value at 12.2 ns. The electrostatic interaction energy developed again since the whole FAD moved closer to the SWNT, forming the second highest electrostatic interaction energy peak around 308.7 kJ mol^{-1} at 13.3 ns. The whole FAD was forced to move away from the SWNT again by the strong electrostatic force while phosphate radical groups got too close to the SWNT. The value of the electrostatic interaction energy dropped to 34.2 kJ mol^{-1} at 15.8 ns while the whole FAD moved the farthest from the SWNT as shown in Fig. 4. Due to the attraction of the deep potential well, FAD moved closer to the SWNT again, making another noticeable peak around 15 ns. Driven by the electrostatic force, FAD moved away from the SWNT. It is obvious that the total interaction energy (black line) and electrostatic interaction energy (red line) curves have very similar trends. The vdW interaction (blue line) gradually decreases during the adsorption process, but the fluctuation is much smaller than that of the total interaction energy, which implies that the vdW interaction contributes a small part of the total interaction. At the final stable state, the total, vdW and electrostatic interaction energies fluctuate around the time-averaged values of 30.0, −0.5, and 30.5 kJ mol^{-1} respectively, and the contribution of the electrostatic interaction to the total is about 98.4%. The snapshots of phosphate radical groups during the simulation were plotted in Fig. 4b and gave a direct view of the distances between the phosphate radical groups and the negatively charged SWNT. This phenomenon implies that it is the orientation of the isoalloxazine and the distance between the negatively charged phosphate radical groups and the negatively charged SWNT that determines the strength of electrostatic interaction between the FAD and the SWNT, the electrostatic interaction plays a key role in the NE-FFS system.

As soon as the MD simulations of the three systems were achieved, the SMD simulations were carried out and the external force was applied to the whole FAD. The stable final states of the three systems were applied as the initial states in SMD simulations respectively. Due to the adsorption of FAD onto the SWNT, the adsorbed groups of the FAD would resist the force applied if the interaction of the specific adsorbed group with the SWNT was larger than the external force. However, other parts of the FAD that are not strongly interacted with the surface moved along the force direction. We went a 400 ps SMD simulation in each system.

The number of adsorbed groups and type of them influence the strength of interaction between FAD and the SWNT, and subsequently influence the desorption behavior of protein from the SWNT. For NU-FFS system in its MD stable state, the groups adsorbed onto the SWNT were isoalloxazine and adenine, which are displayed in notation as initial state of 0 ps in Fig. 6b. The whole FAD moved beneath the surface of the SWNT by the external force in the initial stage of the SMD simulation until the adenine desorbed at about 127 ps. Fig. 6a gives the force-time and the interaction energy–time curves of the SMD simulation. A peak around 127 ps with the external force of 19,570.60 pN is mainly attributed to the resistance of the adenine while the interaction energy raised around −15.58 kJ mol^{-1} as a peak as well. A force peak of 18,508.37 pN around 236 ps was applied to resist the conjugative attraction between isoalloxazine and the SWNT and isoalloxazine finally desorbed around 238 ps, creating an interaction energy peak about 0.71 kJ mol^{-1}. The interaction energy fluctuates around a stable value, indicating that the interaction energy basically is due

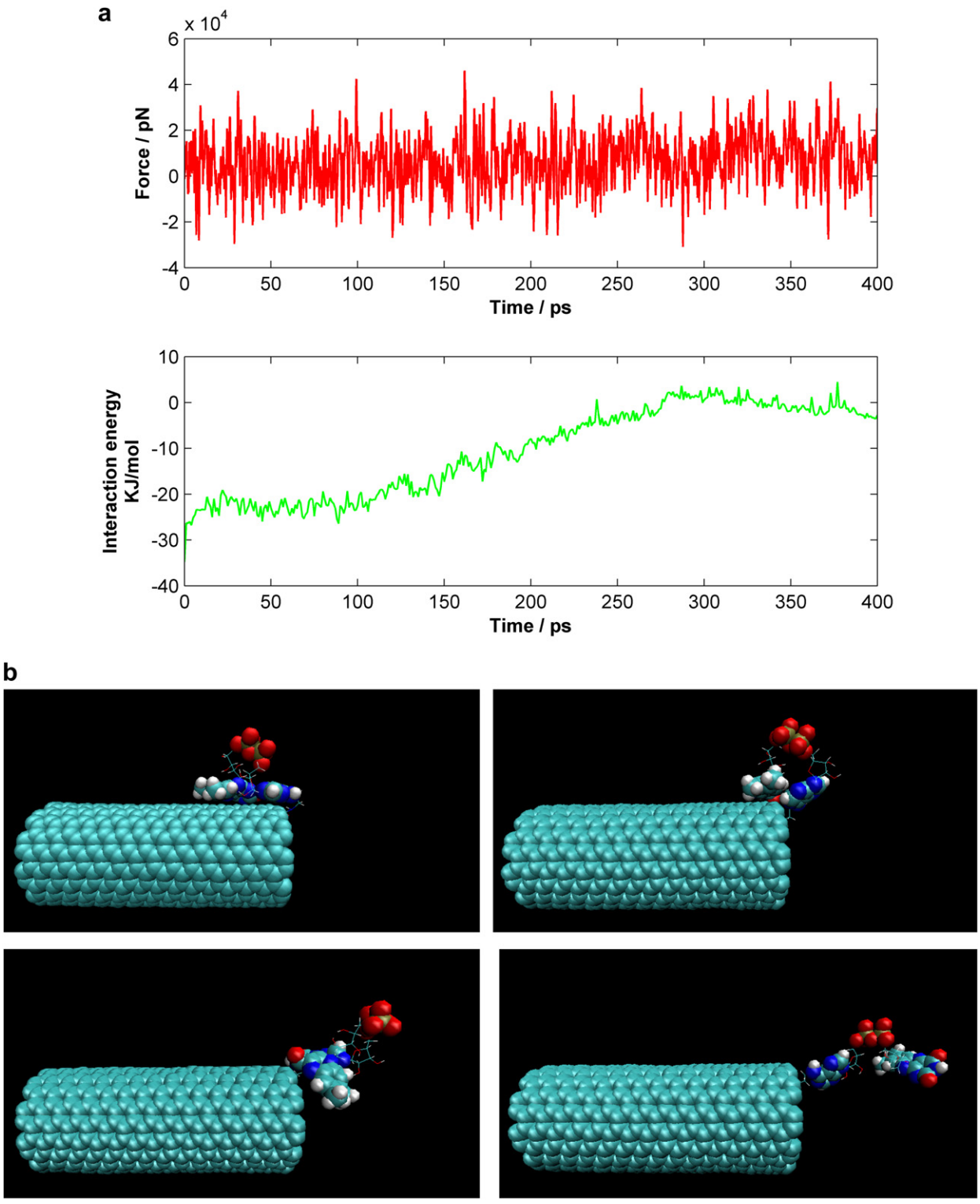

Fig. 6. (a) The interaction energies between FAD and the uncharged SWNT during the SMD simulation.(b) Snapshots of the NU-FFS system (the SWNT, adenine, phosphate radical groups and isoalloxazine displayed by VDW model while other parts of the system displayed by line model) during the SMD simulation. Water molecules and counterions are not displayed here for clarity.

to the adsorption of isoalloxazine and adenine to the surface of the SWNT.

Fig. 7b displays the snapshots of the PO-FFS system in the SMD simulation. In notation of 0 ps in Fig. 7b, the system is in its equilibrium with phosphate radical groups adsorbed onto the SWNT. The FAD moved along the external force, forming a small interaction energy peak around -434.17 kJ mol^{-1} around 96 ps caused by the electrostatic interaction between the positively charged SWNT and the negatively charged oxygen atom in isoalloxazine. However, compared with the strong electrostatic interaction between the

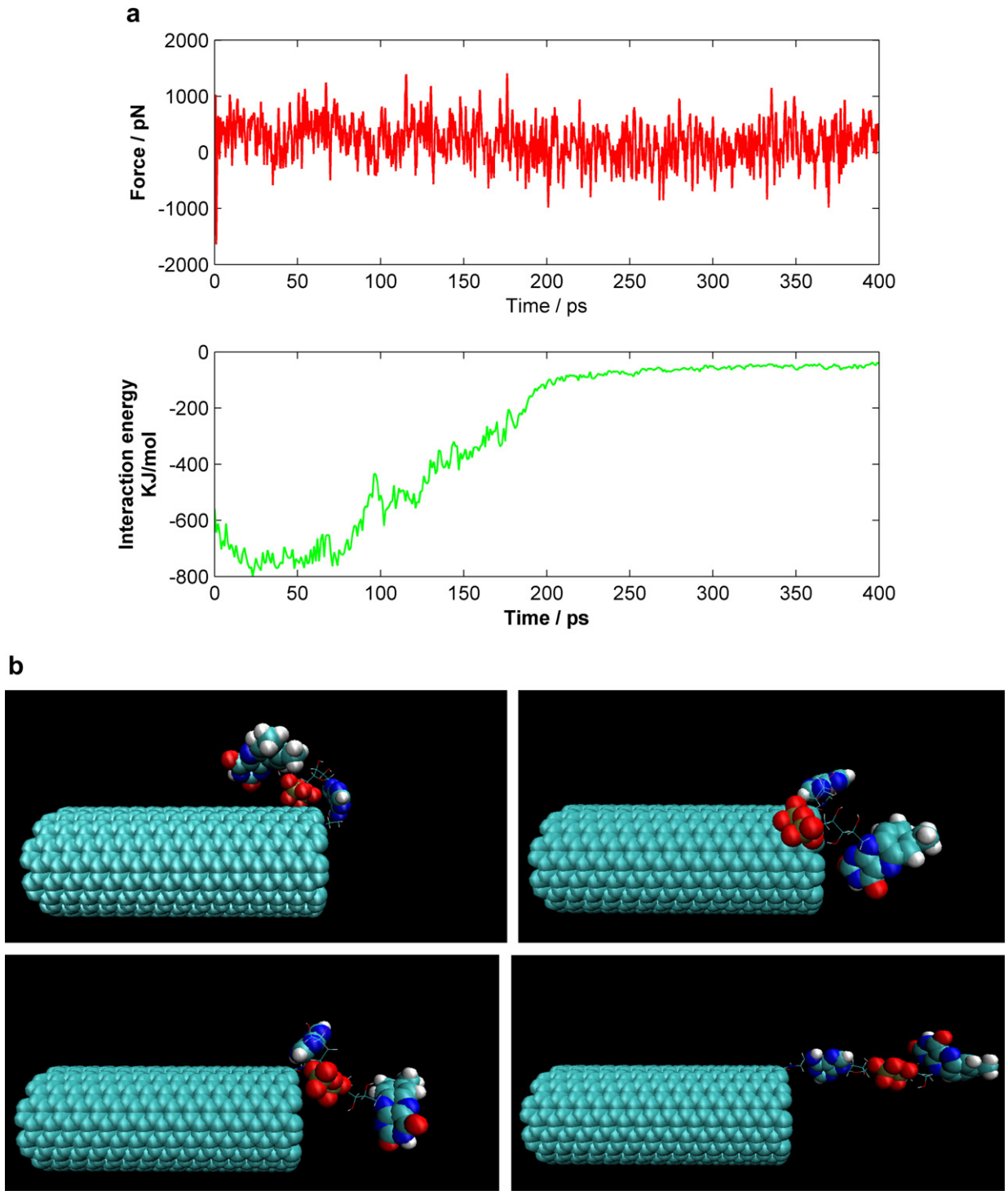

Fig. 7. (a) The interaction energies between FAD and the positively charged SWNT during the SMD simulation. (b) Snapshots of the PO-FFS system (the SWNT, adenine, phosphate radical groups and isoalloxazine displayed by VDW model while other parts of the system displayed by line model) during the SMD simulation. Water molecules and counterions are not displayed here for clarity.

SWNT and the phosphate radical groups, this interaction was relatively smaller. It took more time and larger force to desorb phosphate radical groups. At 187 ps, the phosphate radical groups cannot resist the external force anymore and started to move away from the SWNT. The desorption lasted for about 80 ps. As shown in Fig. 7a, the interaction energy changes mildly around -55 kJ mol^{-1} since 200 ps and reaches -42.99 kJ mol^{-1} at the end of the 400 ps simulation. Evidently, this interaction energy basically is due to the adsorption of the phosphate radical groups onto the SWNT.

For the NE-FFS system, the SMD process was relatively simpler and shorter compared to the ones discussed above. Driven by the external force, the FAD moved away from the SWNT. The SMD simulation lasted 200 ps and the snapshots are displayed in Fig. 8b. The FAD in NE-FFS was already stretched after the MD simulation

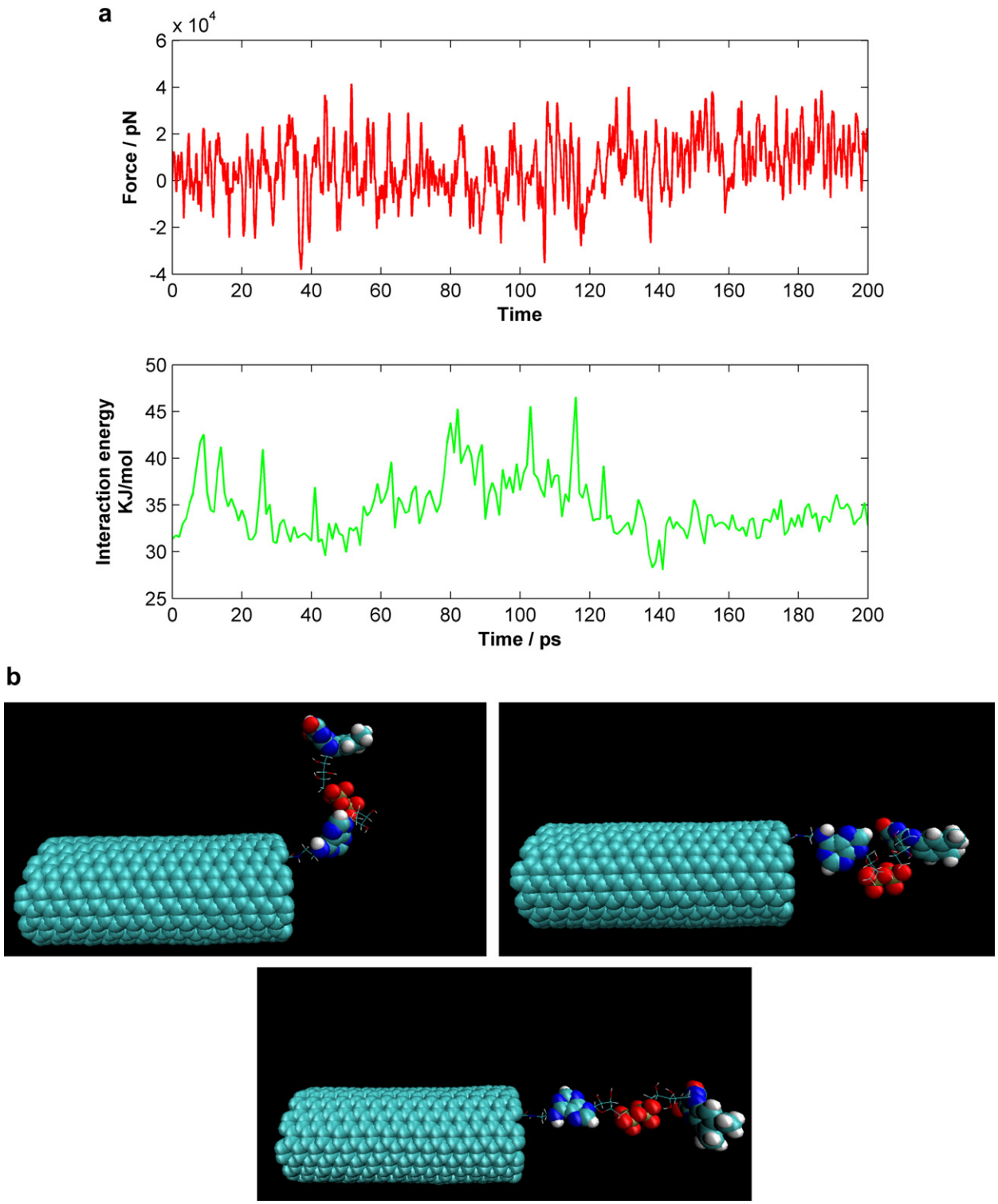

Fig. 8. (a) The interaction energies between FAD and the negatively charged SWNT during the SMD simulation.(b) Snapshots of the NE-FFS system (the SWNT, adenine, phosphate radical groups and isoalloxazine displayed by VDW model while other parts of the system displayed by line model) during the SMD simulation. Water molecules and counterions are not displayed here for clarity.

with no adsorption. Hence, the simulation is less complicated than the other two systems based on the force and interaction energy curves in Fig. 8a.

As illustrated above, the interaction energy strongly depends on the types of groups adsorbed. In order to explore the major attractive force between the FAD and the variously charged SWNT, SMD simulations were carried out. For adsorbed isoalloxazine in the NU-FFS system and phosphate radical groups in the PO-FFS system, the interaction energy varied from -15.29 kJ mol^{-1} to -5.11 kJ mol^{-1} and -532.42 kJ mol^{-1} to -215.89 kJ mol^{-1} respectively. These groups possess the highest ability to adsorb onto the SWNT, which matches the consequences we discussed above in the MD simulations.

In actual experiment circumstances, Itamar Willner and his co-workers have investigated reconstitution of apo-GOx on FAD functionalized SWNT [13]. In our MD runs, we expect the COM distance of FAD and its key part isoalloxazine between SWNT is not too short and it is better that FAD do not adsorb onto exterior surface of SWNT. In other words, because of steric hindrance, the FAD adsorbing onto exterior surface of SWNT can make it harder to be packaged by apo-GOx to form the complete GOx system. According to the analysis above, FAD functionalized on uncharged SWNT is easy to form 'U' shape, and isoalloxazine and adenine are easy to form conjugate structure with the SWNT at the same time. In FAD covalently functionalized positively charged SWNT hybrid system, as the existence of phosphate radical groups with negative charges, the FAD can easily adsorb onto the exterior surface of SWNT. Based on the normalized COM distance data and the simulation trajectory files, it is apparent that FAD in the NE-FFS system stayed the farthest away from SWNT among all three systems. On top of that, FAD in the NE-FFS system remained unfolding in the end of the simulation, and neither isoalloxazine nor phosphate radical groups adsorbed onto SWNT, which gave enough effective space for the GOx reconstitution. So the negatively charged SWNT may be the best choice for constructing the hybrid system for reconstitution of apo-GOx on FAD functionalized SWNT.

In closing, there are still some limitations in these simulations. First, the simulation time scale was not so long enough for a complicated biomolecular system and longer simulations are needed for understanding process of whole system behaviors. And only TIP3 water molecule model was utilized, different water molecule models may also influence the behavior of FAD. Nevertheless, this investigation also achieved some reasonable results.

4. Conclusions

MD and SMD simulations of FAD functionalized variously charged SWNT hybrid systems have been performed. It is found that the different electrical properties of SWNT had different influence on the behaviors of the linked FAD. In the MD simulations, FAD has tendency to get close to the exterior surface of SWNT. Processes of FAD adsorbing onto exterior of differently charged SWNT are distinguished. The adsorption process details were discovered in MD simulations. And the negatively charged SWNT can make the conformation change much smaller than the other two differently charged SWNTs and make FAD much easier to get packaged by apo-GOx. So on actual experiment systems, it is better to construct negatively charged SWNTs to make the conformation of FAD stay stable, FAD activity will also be maintained. The conformation change of different parts of FAD was also investigated. The results showed it was quite different between FAD, isoalloxazine and phosphate radical groups. The conformational change of isoalloxazine was so slight and the structure of isoalloxazine almost stayed the same as its initial state. But comes to FAD, the situation was quite different, and severe distorting of phosphate radical groups and ribitol may be the main reason. This investigation could be helpful to understand the behavior of FAD functionalized differently charged SWNTs, which could be useful for guiding the experiments of the field of glucose oxidase sensors and make contribution to rational design of new biomaterials for next generation biosensors.

Acknowledgments

This work was financially supported by the Nature Science Foundation of Zhejiang Province of China under Grant Z1080300, National Key Technology R&D Program of China (No. 2012BAI16B02), National Natural Science Foundation of China (Nos. 21074115), and funding from Minister of Education of China (Nos. J20091551).

References

[1] Iijima S. Helical microtubules of graphitic carbon. Nature 1991;354:56–8.
[2] Bachtold A, Hadley P, Nakanishi T, Dekker C. Logic circuits with carbon nanotube transistors. Science 2001;294:1317–20.
[3] Baughman RH, Cui C, Zakhidov AA, Iqbal Z, Barisci JN, Spinks GM, et al. Carbon nanotube actuators. Science 1999;284:1340–4.
[4] Derycke V, Martel R, Appenzeller J, Avouris P. Carbon nanotube inter-and intramolecular logic gates. Nano Lett 2001;1:453–6.
[5] Rao C, Satishkumar B, Govindaraj A, Nath M. Nanotubes Chemphyschem 2001;2:78–105.
[6] Tans SJ, Verschueren ARM, Dekker C. Room-temperature transistor based on a single carbon nanotube. Nature 1998;393:49–52.
[7] Boul P, Liu J, Mickelson E, Huffman C, Ericson L, Chiang I, et al. Reversible sidewall functionalization of buckytubes. Chem Phys Lett 1999;310:367–72.
[8] Georgakilas V, Kordatos K, Prato M, Guldi DM, Holzinger M, Hirsch A. Organic functionalization of carbon nanotubes. J Am Chem Soc 2002;124:760–1.
[9] Hirsch A. Functionalization of single-walled carbon nanotubes. Angew Chem Int Ed Engl 2002;41:1853–9.
[10] Liu YC, Shen JW, Gubbins KE, Moore JD, Wu T, Wang Q. Diffusion dynamics of water controlled by topology of potential energy surface inside carbon nanotubes. Phys Rev B 2008;77:125438.
[11] Zhao W, Song C, Pehrsson PE. Water-soluble and optically pH-sensitive single-walled carbon nanotubes from surface modification. J Am Chem Soc 2002; 124:12418–9.
[12] Katz E, Riklin A, Heleg-Shabtai V, Willner I, Bückmann A. Glucose oxidase electrodes via reconstitution of the apo-enzyme: tailoring of novel glucose biosensors. Anal Chim Acta 1999;385:45–58.
[13] Patolsky F, Weizmann Y, Willner I. Long-range electrical contacting of redox enzymes by SWCNT connectors. Angew Chem Int Ed Engl 2004;43:2113–7.
[14] Karplus M, McCammon JA. Molecular dynamics simulations of biomolecules. Nat Struct Biol 2002;9:646–52.
[15] Katz E, Willner I. Biomolecule-functionalized carbon nanotubes: applications in nanobioelectronics. Chemphyschem 2004;5:1084–104.
[16] Shen JW, Wu T, Wang Q, Kang Y. Induced stepwise conformational change of human serum albumin on carbon nanotube surfaces. Biomaterials 2008;29: 3847–55.
[17] Zhao X, Johnson JK. Simulation of adsorption of DNA on carbon nanotubes. J Am Chem Soc 2007;129:10438–45.
[18] Keblinski P, Nayak S, Zapol P, Ajayan P. Charge distribution and stability of charged carbon nanotubes. Phys Rev Lett 2002;89:255503.
[19] Luo J, Peng LM, Xue Z, Wu J. Density-functional-theory calculations of charged single-walled carbon nanotubes. Phys Rev B 2002;66:115415.
[20] Simonyan VV, Diep P, Johnson JK. Molecular simulation of hydrogen adsorption in charged single-walled carbon nanotubes. J Chem Phys 1999;111:9778.
[21] Lee R, Kim H, Fischer J, Thess A, Smalley RE. Conductivity enhancement in single-walled carbon nanotube bundles doped with K and Br. Nature 1997; 388:255–6.
[22] Rao A, Eklund P, Bandow S, Thess A, Smalley RE. Evidence for charge transfer in doped carbon nanotube bundles from Raman scattering. Nature 1997;388:257–9.
[23] Javey A, Tu R, Farmer DB, Guo J, Gordon RG, Dai H. High performance n-type carbon nanotube field-effect transistors with chemically doped contacts. Nano Lett 2005;5:345–8.
[24] Gong K, Du F, Xia Z, Durstock M, Dai L. Nitrogen-doped carbon nanotube arrays with high electrocatalytic activity for oxygen reduction. Science 2009; 323:760–4.
[25] Biswas C, Lee SY, Ly TH, Ghosh A, Dang QN, Lee YH. Chemically doped random network carbon nanotube p-n junction diode for rectifier. ACS Nano 2011;5: 9817–23.
[26] Deng C, Chen J, Chen X, Xiao C, Nie L, Yao S. Direct electrochemistry of glucose oxidase and biosensing for glucose based on boron-doped carbon nanotubes modified electrode. Biosens Bioelectron 2008;23:1272–7.
[27] Talla JA. First principles modeling of boron-doped carbon nanotube sensors. Physica B Condens Matter 2012;407:966–70.
[28] Cruz-Silva E, Cullen DA, Gu L, Romo-Herrera JM, Muñoz-Sandoval E, López-Urías F, et al. Heterodoped nanotubes: theory, synthesis, and characterization of phosphorus-nitrogen doped multiwalled carbon nanotubes. ACS Nano 2008;2:441–8.
[29] Kim SM, Jang JH, Kim KK, Park HK, Bae JJ, Yu WJ, et al. Reduction-controlled viologen in bisolvent as an environmentally stable n-type dopant for carbon nanotubes. J Am Chem Soc 2008;131:327–31.
[30] Kang BR, Yu WJ, Kim KK, Park HK, Kim SM, Park Y, et al. Restorable type conversion of carbon nanotube transistor using pyrolytically controlled anti-oxidizing photosynthesis coenzyme. Adv Funct Mater 2009;19:2553–9.
[31] Hecht H, Kalisz H, Hendle J, Schmid R, Schomburg D. Crystal structure of glucose oxidase from aspergillus niger refined at 2.3 Å resolution. J Mol Biol 1993;229:153–72.
[32] MacKerell Jr AD, Bashford D, Bellott M, Dunbrack Jr RL, Evanseck J, Field M, et al. All-atom empirical potential for molecular modeling and dynamics studies of proteins. J Phys Chem B 1998;102:3586–616.
[33] Humphrey W, Dalke A, Schulten K. VMD: visual molecular dynamics. J Mol Graph 1996;14:33–8.
[34] Shen JW, Wu T, Wang Q, Pan HH. Molecular simulation of protein adsorption and desorption on hydroxyapatite surfaces. Biomaterials 2008;29:513–32.

[35] Wilson R, Turner A. Glucose oxidase: an ideal enzyme. Biosens Bioelectron 1992;7:165–85.
[36] Degani Y, Heller A. Direct electrical communication between chemically modified enzymes and metal-electrodes. 1. electron-transfer from glucose oxidase to metal-electrodes via electron relays, bound covalently to the enzyme. J Phys Chem 1987;91:1285–9.
[37] Schuhmann W, Ohara TJ, Schmidt HL, Heller A. Electron transfer between glucose oxidase and electrodes via redox mediators bound with flexible chains to the enzyme surface. J Am Chem Soc 1991;113:1394–7.
[38] Willner I, Katz E. Integration of layered redox proteins and conductive supports for bioelectronic applications. Angew Chem Int Ed Engl 2000;39:1180–218.
[39] Willner I, Riklin A, Shoham B, Rivenzon D, Katz E. Development of novel biosensor enzyme electrodes: glucose oxidase multilayer arrays immobilized onto self-assembled monolayers on electrodes. Adv Mater 1993;5:912–5.
[40] Gerard M, Chaubey A, Malhotra B. Application of conducting polymers to biosensors. Biosens Bioelectron 2002;17:345–59.
[41] Alexiadis A, Kassinos S. Molecular simulation of water in carbon nanotubes. Chem Rev 2008;108:5014.
[42] Tatke S, Renugopalakrishnan V, Prabhakaran M. Interfacing biological macromolecules with carbon nanotubes and silicon surfaces: a computer modelling and dynamic simulation study. Nanotechnology 2004;15: S684–90.